Lasers in Surgery and Medicine 22:14–24 (1998)

Subcellular Phototoxicity of 5-Aminolaevulinic Acid (ALA)

Hong Liang, PhD, David S. Shin, Yider Eddie Lee, Duc Chi Nguyen, Tina Ching Trang, Ann Huang Pan, Scott Li-Ju Huang, David Huber Chong, and Michael W. Berns, PhD*

Beckman Laser Institute and Medical Clinic, University of California, Irvine, Irvine, California 92612

Background and Objective: **5-aminolaevulinic acid (ALA) is a new, promising photosensitizer for PDT of cancer. Subcellular toxicity induced by ALA and light exposure in single cells was studied to elucidate the mechanism of cell damage.**
Study Design/Materials and Methods: **CPAE, PTK_2, and rat neonatal myocardial cells treated with ALA were examined for localization using fluorescence microscopy and for subcellular phototoxicity using 630 nm laser microbeam irradiation of specific subcellular regions.**
Results: **In CPAE and PTK_2 cells, a large amount of fluorescence was detected in the peri-nuclear cytoplasm. In rat neonatal myocardial cells, the sensitizer selectively localized in the large mitochondria. In both cell types, there was little phototoxicity when the peripheral cytoplasmic region was exposed, as compared to considerable phototoxicity with exposure of either the perinuclear or nuclear regions.**
Conclusion: **Both the CPAE and PTK_2 cells demonstrated that the nucleus followed by the perinuclear cytoplasm are the most sensitive cell areas with no sensitivity in the peripheral cytoplasm. Lasers Surg. Med. 22:14–24, 1998.** **© 1998 Wiley-Liss, Inc.**

Key words: endothelial cell; fluorescence detection; laser microirradiation; photodynamic therapy; photosensitizer

INTRODUCTION

Photodynamic therapy (PDT) of malignant tumors is a modality that involves the irradiation of tumors with light following selective uptake of a photosensitizer by the tumor tissue [1]. 5-aminolaevulinic acid (ALA) is a precursor in the biosynthesis of heme, cytochrome, chlorophyll, bile pigments and other porphyrins. It is converted intracellularly to monomeric protoporphyrin IX which has a high fluorescence yield, and strong photosensitizing capability [2]. Introduced by Kennedy [3,4], ALA has become a promising agent for PDT as it can be delivered topically and orally, and causes skin photosensitivity only for a short period of time [5,6].

Vascular destruction may be a major component of PDT. It may be caused by the collapse and/or breakdown of the tumor microvasculature following light exposure [7,8]. The vascular endothelium within a tumor shows distinct changes immediately after PDT [9]. It has been suggested that in PDT-treated tumors, the vascular endothelium is damaged initially while tumor cells are destroyed secondarily as a result of structural damage to capillaries and functional disturbance in the microcirculation [8,9]. It has been sug-

Contract grant sponsor: NIH; Contract grant numbers: RO1CA32248, RR01192; Contract grant sponsor: Office of Naval Research; Contract grant number: ONR N00014-91-C-0134; Contract grant sponsor: Department of Energy; Contract grant number: DE-F03-91ER61227; Contract grant sponsor: Beckman Laser Institute Endowment.

*Correspondence to: Dr. Michael W. Berns, Beckman Laser Institute and Medical Clinic, University of California at Irvine, 1002 Health Sciences Road East, Irvine, CA 92612.

Accepted 10 October 1997

gested that endothelial cell death may be a consequence of direct cell injury resulting from retention of photosensitizer within the endothelial cell or, alternately, result from intravascular activation of circulating photosensitizer with subsequent indirect damage to the endothelial cell [10].

Although it is clear that endothelial cells play a crucial role in PDT-induced tumor destruction, the exact nature of the endothelial cell damage is not well known. In this paper we employ laser microirradiation of specific subcellular regions in combination with low light level fluorescence detection to elucidate the mechanism of PDT.

MATERIALS AND METHODS

Cells and Cell Culture

Three cell types were used in these studies. Bovine pulmonary artery endothelium cells (CPAE) were obtained from the American Type Culture Collection (ATCC). This is an endothelial cell line derived from the main stem pulmonary artery of a young, female cow (*Box taurus*). The cells were grown in Eagle's minimal essential medium with 20% fetal bovine serum in a 37°C and 5–7% CO_2 atmosphere. The cells were maintained and subcultured approximately 2–3 weeks before being discarded and replaced with fresh cells from the same passage.

Rat kangaroo kidney cells (*Potorous tridactylis*) (PTK_2) were originally obtained from ATCC and grown as a monolayer in a modified Eagle's minimal essential medium with 10% fetal bovine serum. The cells were subcultured once a week into T-25 culture flask and maintained in a 37°C and 5–7% CO_2 incubator. These cells are thin and remain relatively flat throughout the cell cycle, permitting clear visualization of the subcellular morphology.

Twenty four hours prior to the experiments, the cells were injected into standard Rose culture chambers at a density of ~1×10^3 cells/ml. Four hours prior to laser microirradiation, the cells were exposed to fresh culture medium containing 50 μg/ml ALA. Cells without exposure to ALA served as controls. The chambers were covered with aluminum foil immediately after injecting medium with ALA in order to prevent the cells from ambient light exposure. Individual healthy cells were selected under the phase contrast microscope and identified for the light-exposure experiment by placing a circle around them on the outer surface of the Rose chamber glass window with a Zeiss diamond objective. Cells that did not have any neighboring cells within the marked circle were chosen. The same criteria for cell selection was applied to experimental and control cells. Primary culture neonatal rat myocardial cells were exposed to the ALA in order to visualize subcellular fluorescence [11]. These cells were obtained from Dr. Joe Bahl, University Heart Center, University of Arizona. The cells were prepared by serial digestion with viokase and preplated to remove fibroblasts. The cells were injected into Rose chambers after adjusting to approximately 2.5×10^5 cells/ml in defined Eagle's minimal essential medium with 10% FBS + penicillin and streptomycin. Forty eight hours later the medium was changed to defined MEM with 1% FBS + penicillin and streptomycin. The medium was changed every 3–4 days. Healthy contracting myocardial cells were observed for 3–4 weeks.

A Coherent (Palo Alto, CA) Model 210 power meter was used to measure the power at the entrance to the objective. To determine the actual power reaching the irradiated sample, the dual objective transmittance measuring technique of Misawa et al. [12] was used. This method eliminates total internal reflection errors that are encountered in a direct objective-to-power measurement in air. Using this method it was determined that each cell was exposed to 140mW of power at a power density of 7.2×10^7 W/cm^2. The total energy densities (fluence) per experiment were obtained by varying time exposure. The parameters used are listed in Table 1. Immediately before laser irradiation of each cell, a phase contrast image of the cell was made using the CCD camera. Each chamber was labeled and placed back into the CO_2 incubator after the irradiation. Each cell was followed and recorded morphologically at 24 hours and 48 hours after the initial irradiation.

Fluorescence Microscopy

A Zeiss Axiovert inverted fluorescence microscope (Thornwood, NY) was used for fluorescence detection. ALA-treated cells were tested for fluorescence at 1 hour intervals from 4 to 7 hours after the initial administration of the photosensitizer. Each individual cell was excited with UV light ($\lambda = 365$) using a 100 W arc lamp. An image was recorded of the fluorescence within the cell using a cooled charge-couple device (CCD) (Princeton Instruments TE/CCD- 576E/UV) and stored in IP Lab format in a Macintosh IIfx com-

TABLE 1. Some Parameters Utilized in Laser Microirradiation Experiments

	Power (mW)	140	140	140	140	140
CPAE	Power density (W/cm^2)	7.2×10^7	7.2×10^7	7.2×10^7	7.2×10^7	7.2×10^7
	Time exposure (sec)	600	480	300	240	180
	Energy density (J/cm^2)	4.4×10^{10}	3.4×10^{10}	2.2×10^{10}	1.7×10^{10}	1.2×10^{10}
PTK_2	Power density (W/cm^2)	7.2×10^7	7.2×10^7	7.2×10^7	7.2×10^7	7.2×10^7
	Time exposure (sec)	100	30	20	10	5
	Energy Density (J/cm^2)	7.2×10^9	2.2×10^9	1.4×10^9	0.72×10^9	0.36×10^9

puter. A phase contrast picture of each cell was also taken for reference. Images were digitally rendered improving contrast and reducing background light.

Microirradiation of Subcellular Components

A laser microbeam system was used that employed an argon ion laser (Coherent Innova 90) pumped dye laser (Coherent 599 dye) to generate a 630 nm beam. The beam was directed through a Zeiss Axiovert inverted microscope using a Zeiss Neofluar 100× phase contrast objective having a numerical aperture of 1.3. For each cell, the laser beam was focused upon either the center of the nucleus, the perinuclear cytoplasm, or the peripheral cytoplasm. The cytoplasm just above the nucleus was also exposed in some experiments. The laser spot was approximately 0.5 μ in diameter.

A Coherent (Palo Alto, CA) Model 210 power meter was used to measure the power at the entrance to the objective. To determine the actual power reaching the irradiated sample, the dual objective transmittance measuring technique of Misawa et al. [12] was used. This method eliminates total internal reflection errors that are encountered in a direct objective-to-power measurement in air. Using this method it was determined that each cell was exposed to 140 mW of power at a power density of 7.2×10^7 W/cm^2. The total energy densities (fluence) per experiment were obtained by varying time exposure. The parameters used are listed in Table 1.

Immediately before laser irradiation of each cell, a phase contrast image of the cell was made using the CCD camera. Each chamber was labeled and placed back into the CO_2 incubator after the irradiation. Each cell was followed and recorded morphologically at 24 hours and 48 hours after the initial irradiation.

RESULTS

Fluorescence Detection

CPAE and PTK_2 cells. Fluorescence in untreated control cells and ALA-treated CPAE and PTK_2 cells was examined and recorded using the CCD system. Figure 1a is a phase contrast image of a control untreated CPAE cell and Figure 1b is a fluorescence image of the same cell demonstrating a few concentrated areas of autofluorescence. Figure 1c and 1d are paired images of a CPAE cell 4 hours following exposure to 50 μg/ml ALA demonstrating a large amount fluorescence in the peri-nuclear cytoplasm that extends somewhat out to the periphery of the cell. However, careful comparison with the adjacent phase contrast image (Figure 1c) illustrates that most of the peripheral cytoplasm is devoid of fluorescence.

Control PTK_2 cells (Figs. 2a and 2b) demonstrate no detectable autofluorescence. The ALA-treated cells (Figs. 2c and 2d) exhibit heavy diffuse fluorescence in the perinuclear cytoplasm 4 hours after exposure to 50 μg ALA. No intranuclear fluorescence was detected in either the CPAE or PTK2 cells.

Myocardial cells. In the neonatal myocardial cells treated with 50 μg/ml of ALA, the sensitizer selectively localizes in the large mitochondria (Figs. 3a and 3b).

Subcellular Phototoxicity After Laser Microirradiation

In all of the subcellular microirradiation studies a laser power of 140 Mw (7.2×10^7W/cm^2) at the microscope objective focal point was used. The total energy densities (ED) were varied by changing the duration of laser exposure (Table 1).

CPAE cells. A total of 232 CPAE cells were irradiated in the following subcellular regions: nucleus (Figs. 4a and c) n = 80; perinuclear cytoplasm (Figs. 5a, c and 6a, c), n = 77; peripheral cytoplasm (Fig. 7a), n = 39; cytoplasm above nucleus, (no figure is available because the location was the same as the nuclear exposure except the cell image was defocused so that the focal plane of the laser spot was in the cytoplasm region above the nucleus), n = 16; control microscope illumination, n = 20. The locations of the laser microspot in each cell regions, except in the last two, are depicted in the above referenced fig-

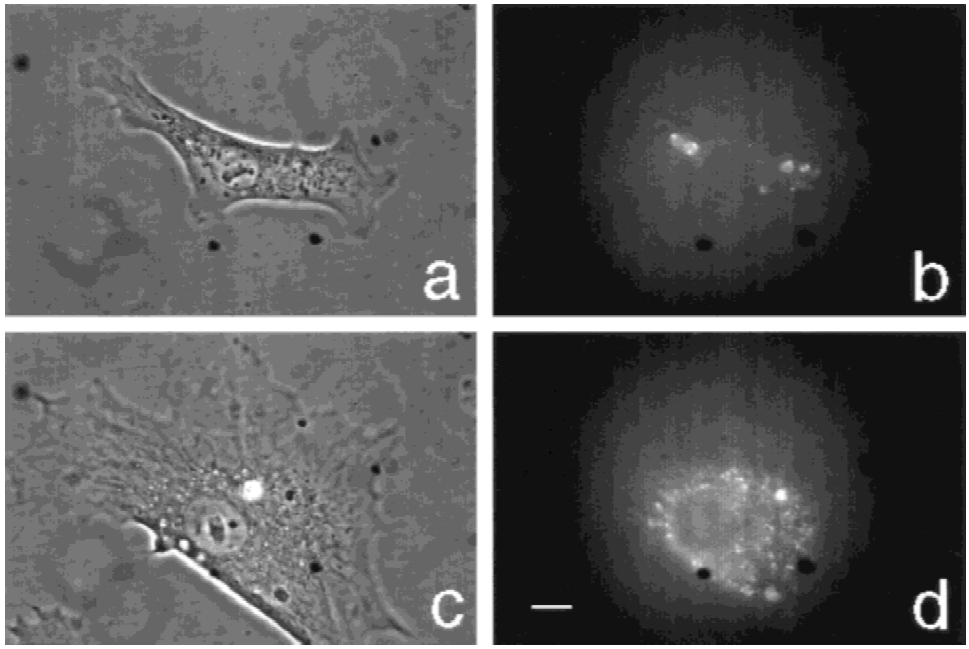

Fig. 1. Fluorescence image of CPAE cells treated by ALA. (**a**) Phase contrast image of control single cell without ALA treatment. (**b**) Fluorescence image of the same cell. (**c**) Phase contrast image of single cell 4 hours after treatment with ALA. (**d**) Fluorescence image of the same cell. Scale bar, 10 μm.

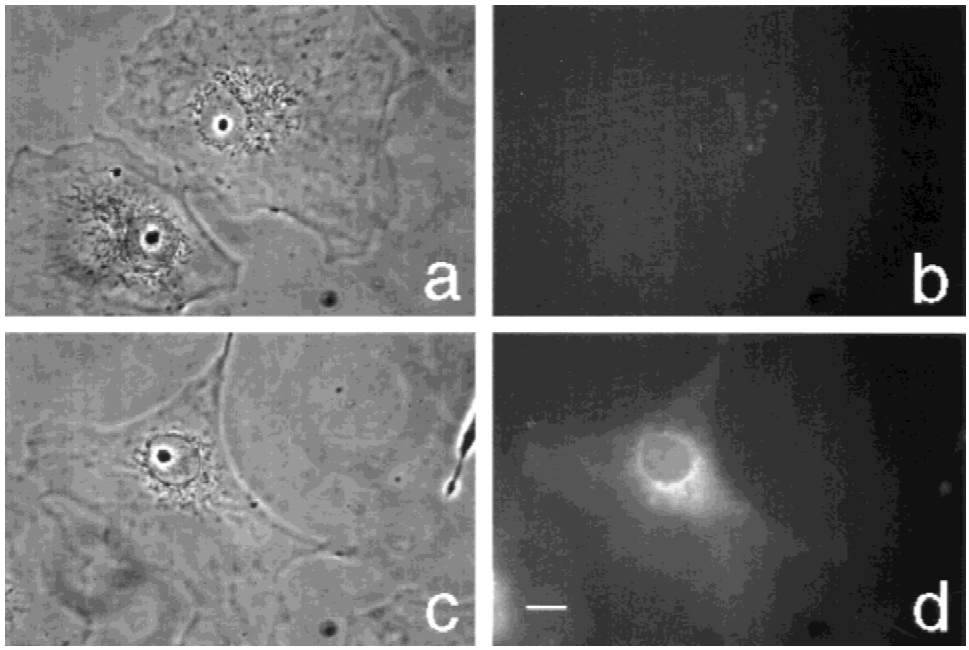

Fig. 2. Fluorescence image of PTK_2 cells treated by ALA. (**a**) Phase contrast image of control single cell without ALA treatment. (**b**) Fluorescence image of the same cell. (**c**) Phase contrast image of single cell 4 hours after treatment with ALA. (**d**) Fluorescence image of the same cell. Scale bar, 10 μm.

ures. The subsequent corresponding photograph for each of the above cells (i.e., Figures "b" and "d") illustrate the ultimate fate of that cell 24 or 48 hours after laser exposure.

Cells at 24 and/or 48 hours post microirradiation were categorized as follows: (1) healthy and undergoing at least one mitotic event (see Fig. 7b); (2) morphologically normal but not having undergone an additional cell division (see Fig. 5b); (3) aberrant giant cells containing a large vol-

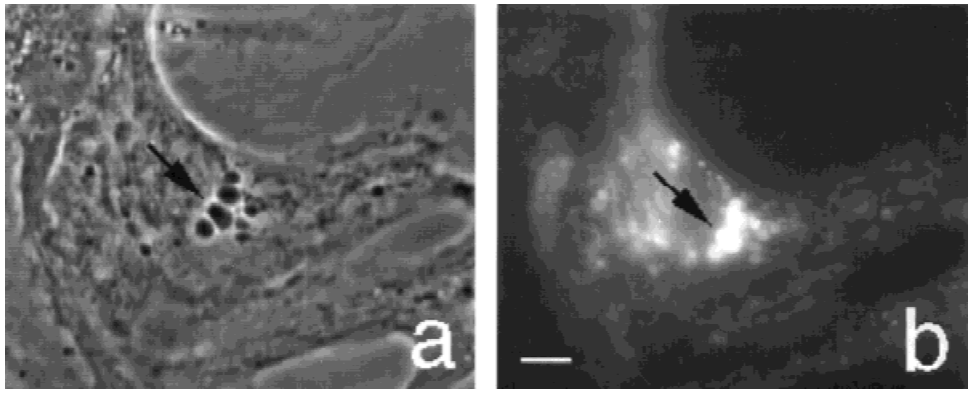

Fig. 3. Fluorescence image of neonatal rat myocardial cells treated by ALA. (**a**) Phase contrast image of single cell 4 hours after treatment with ALA. (**b**) Fluorescence image of the same cell. Scale bar, 10 μm.

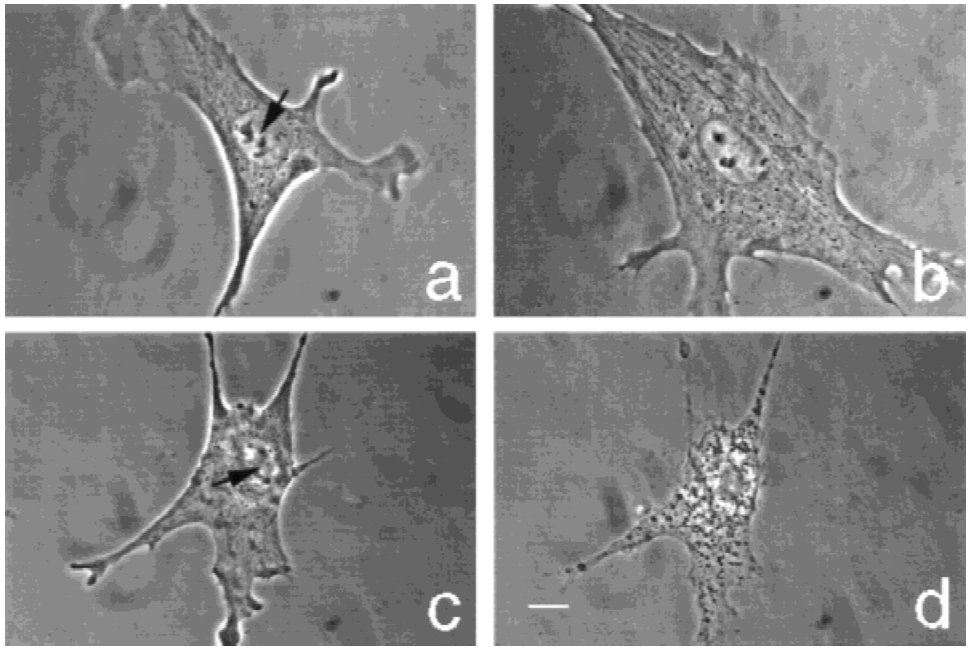

Fig. 4. Cellular damage in single CPAE cells after laser microirradiation onto nucleus. (**a**) A single cell without ALA treatment just before laser microirradiation. Arrow denotes the target ready to trigger. (**b**) The same cell 24 hours after 5 minutes of laser irradiation onto nucleus. (**c**) A single cell with ALA treatment just before laser microirradiation. Arrow denotes the target ready to trigger. (**d**) The same cell 24 hours after 5 minutes of laser irradiation onto nucleus. Scale bar, 10 μm.

ume of cytoplasm (see Figure 5d) or multi-nuclei; (4) cells that appeared vacuolated, disintegrating, and often lysed (see Fig. 4b). Only the first two cell types were considered to be healthy.

Figure 8 is a graph of the cumulative data depicting the percentage of damaged CPAE cells following exposure to different subcellular regions with different total energy doses (as a function of exposure time). It is clear that there is little phototoxicity when the peripheral cytoplasmic is exposed. There is considerable phototoxicity with exposure of either the perinuclear or nuclear regions, with the latter being the most sensitive target site. The raw data is provided in Table 2. In this table, each cell region and light dose (time of exposure) are included for experimental cells where light and drug were applied, and control cells involving light alone. Control cells treated with drug alone were also studied, but are not presented in the raw data. No adverse effects were seen on cells in this control group (see previous fluorescence detection section).

Of particular interest is that the control (non-ALA) cells exhibited significant adverse ef-

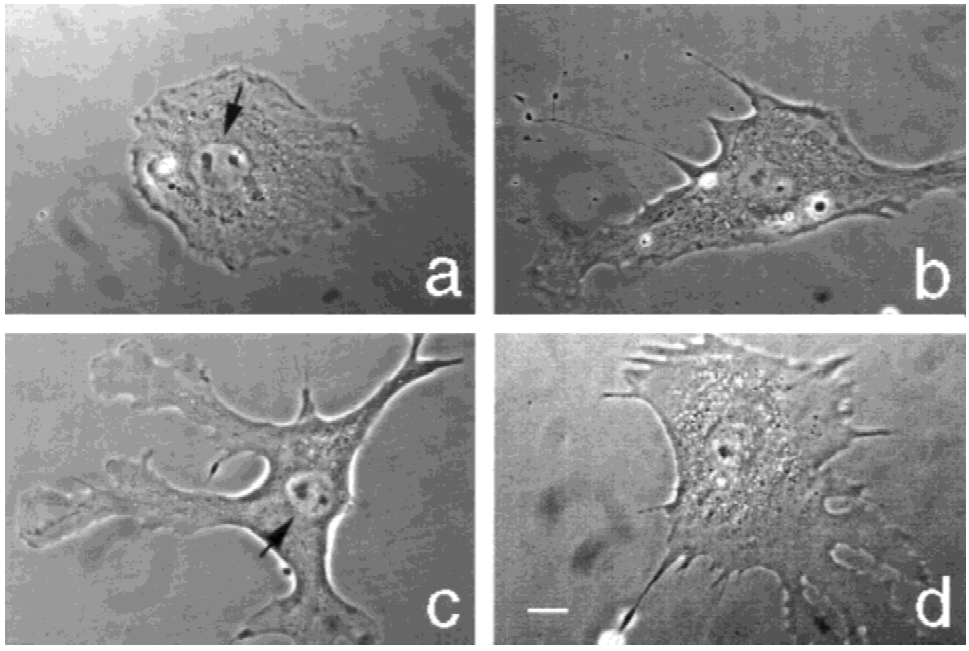

Fig. 5. Cellular damage in single CPAE cells after laser microirradiation onto perinuclear cytoplasm. (**a**) A single cell without ALA treatment just before laser microirradiation. Arrow denotes the target ready to trigger. (**b**) The same cell, 24 hours after 8 minutes of laser microirradiation onto perinuclear cytoplasm. (**c**) A single cell pretreated with ALA just before laser microirradiation. Arrow denotes the target ready to trigger. (**d**) The same cell, 24 hours after 8 minutes of laser microirradiation onto perinuclear cytoplasm. Scale bar, 10 μm.

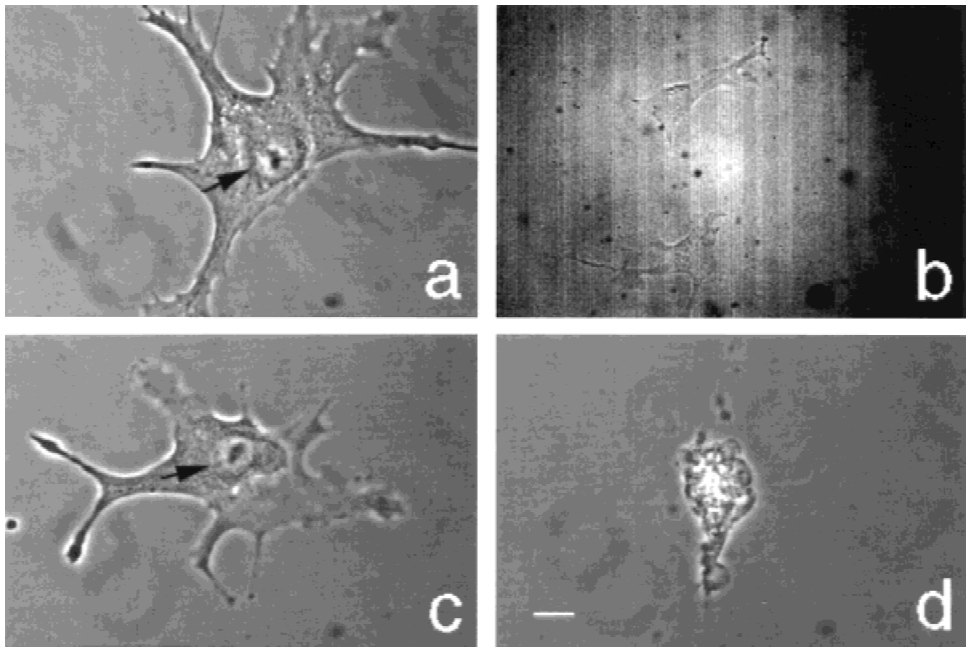

Fig. 6. Cellular damage in single CPAE cells after laser microirradiation onto perinuclear cytoplasm. (**a**) A single cell without ALA treatment just before laser microirradiation. Arrow denotes the target ready to trigger. (**b**) The cell divided into 2 cells at 24 hours after 5 minutes of laser microirradiation onto perinuclear cytoplasm (picture taken under x40 objective). (**c**) A single cell pretreated with ALA just before laser microirradiation. Arrow denotes the target ready to trigger. (**d**) The same cell lysed 24 hours after 5 minutes laser microirradiation onto perinuclear cytoplasm. Scale bar, 10 μm.

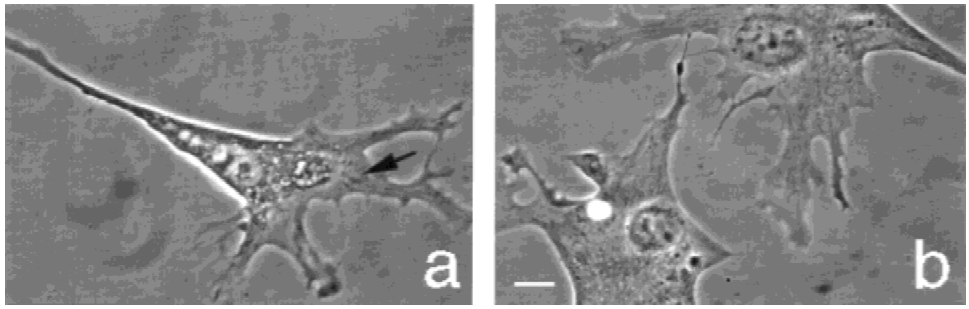

Fig. 7. Results of laser microirradiation of peripheral cytoplasm in CPAE cells with pretreatment of ALA. (**a**) A single cell pretreatment with ALA before laser irradiation. Arrow denotes the target ready to trigger. (**b**) Formation of two daughter cells 24 hours after 5 minutes of laser microirradiation of peripheral cytoplasm. Scale bar, 10 μm.

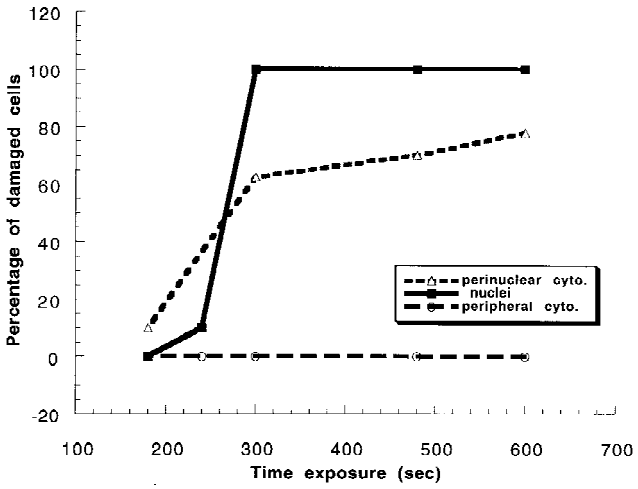

Fig. 8. Cellular toxicity at 24 hours after subcellular laser microirradiation in CPAE cells treated with ALA.

fects to the longer nuclear irradiations assayed at both 24 and 48 hours post exposure. At 24 hours post light exposure of 10 and 5 minutes, 90% and 25% of the cells exhibited damage. At 48 hours post light exposure, cell damage was observed in 90% and 75% of the cells treated with light alone for 10 and 5 minutes respectively. ALA-treated cells exhibited 100% cell damage at all time regimes of light exposure.

Not shown on the graph (but included in Table 2) is an experiment where the cytoplasm directly above the nucleus (supranuclear) was irradiated for 5 minutes with the same amount of power as used in all the experiments (140 mW). The percentage of damaged cells was 20% and 30% for 24 and 48 hours post light exposure. This compares to 100% damaged cells for nuclear exposure at both 24 and 48 hours, and 62% and 75% damaged cells for 24 and 48 hours post light exposure to the perinuclear cytoplasm.

CPAE cells subjected only to microscope illumination were also studied to verify if there was any adverse effect on cell survival. Perinuclear cytoplasm in 10 cells with ALA treatment and 10 cells without ALA treatment were exposed to 10 minutes of microscope illumination. All the cells in both groups were viable and healthy after 24 and/or 48 hours. The data from the graphs (Fig. 8) suggest a decreasing order of subcellular sensitivity in ALA-treated cells as follows: nucleus, perinuclear cytoplasm, and peripheral cytoplasm.

PTK_2 cells. A total of 277 cells were exposed to the laser microbeam. A graph summarizing these results is presented in Figure 11. The greatest sensitivity is in the nucleus, followed by the perinuclear cytoplasm, and peripheral cytoplasm. The raw data are presented in Table 3. The pre-exposure and post irradiation cell morphology are presented in Figures 9 and 10.

All of the cell regions in ALA-treated cells were much more sensitive (by an order of magnitude of light dose) to the light exposure than the same regions in the CPAE cells. In addition, no control light-alone exposure to the nucleus resulted in cell damage. This is in major contrast to the CPAE cells. Supranuclear/subnuclear cytoplasm was not exposed in PTK2 cells.

DISCUSSION

The fluorescence data in both the CPAE and PTK_2 cells demonstrated a selective concentration of protoporphyrin IX in the perinuclear region of the cytoplasm. The fluorescence results in the neonatal myocardial cells clearly showed that the sensitizer was bound selectively to the mitochondria. However, since there is some diffuse fluorescence in other region of the cytoplasm, some binding of other organelles or nonspecific binding can not be entirely ruled out. In all three

TABLE 2. Cell Status Morphologically in CPAE After Treatment of ALA Plus Laser Microirradiation

Target of irradiation	Pretreatment of ALA	Time of exposure (min)	Total no. of cells attempted	Cell status after 24 hours				Cell status after 48 hours			
				Healthy cells[a]		Damaged cells[b]		Healthy cells[a]		Damaged cells[b]	
				No.	%	No.	%	No.	%	No.	%
Nucleus	no	10	10	1	10	9	90	1	10	9	90
	yes	10	5	0	0	5	100	0	0	5	100
	no	8	10	5	50	5	50				
	yes	8	5	0	0	5	100	0	0	5	100
	no	5	8	6	75	2	25	2	25	6	75
	yes	5	10	0	0	10	100	0	0	10	100
	no	4	6	6	100	0	0	6	100	0	0
	yes	4	10	9	90	1	10	7	70	3	30
	no	3	6	6	100	0	0	6	100	0	0
	yes	3	10	10	100	0	0	10	100	0	0
Perinuclear cytoplasm	no	10	13	13	100	0	0	13	100	0	0
	yes	10	9	2	22	7	78	2	22	7	78
	no	8	8	8	100	0	0	8	100	0	0
	yes	8	10	3	30	7	70	3	30	7	70
	no	5	10	10	100	0	0	10	100	0	0
	yes	5	8	3	38	5	62	2	25	6	75
	no	3	9	9	100	0	0	9	100	0	0
	yes	3	10	9	90	1	10	9	90	1	10
Peripheral cytoplasm	no	10	10	10	100	0	0	10	100	0	0
	yes	10	9	9	100	0	0	8	89	1	11
	yes	8	5	5	100	0	0	5	100	0	0
	no	5	8	8	100	0	0	8	100	0	0
	yes	5	7	7	100	0	0	7	100	0	0
Cytoplasm above nuclear membrane	no	5	6	6	100	0	0	6	100	0	0
	yes	5	10	8	80	2	20	7	70	3	30

[a]Healthy cells: Cells underwent at least one additional mitosis and cells with no division but morphologically normal, alive and healthy.
[b]Damaged cells: Cells morphologically aberrant such as with large volume or multi-nuclei and cells vacuolated, disintegrated and lysed.

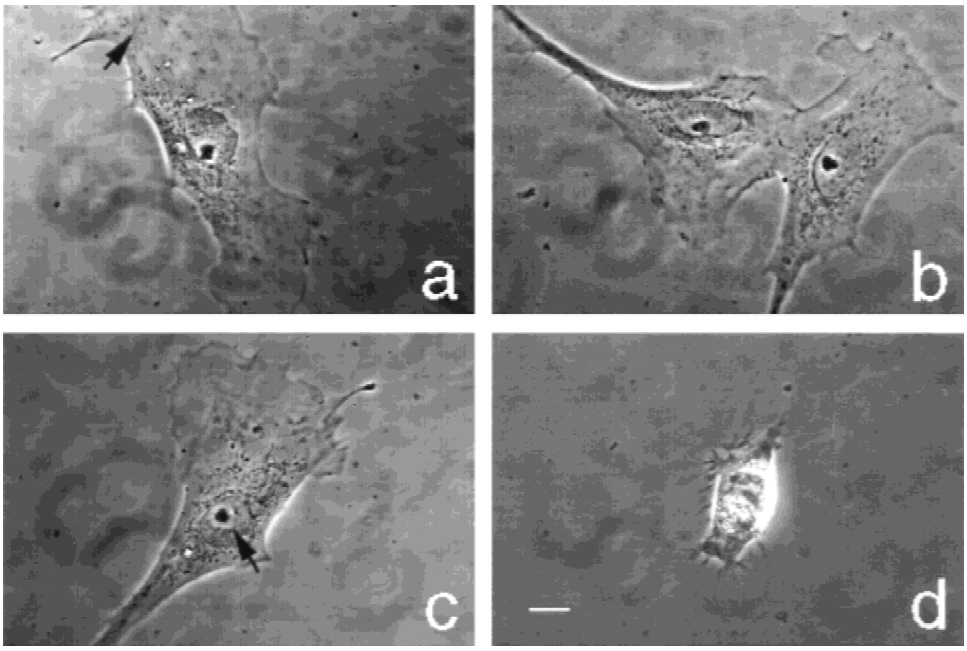

Fig. 9. Cellular damage in single PTK_2 cell after pretreatment of ALA and laser microirradiation. (**a**) A single cell pretreated with ALA ready to irradiate. Arrow denotes the target of peripheral cytoplasm location. (**b**) The cell underwent mitosis, and two daughter cells produced 24 hours after 30 sec of laser microirradiation. (**c**) A single cell pretreated with ALA ready to irradiate. Arrow denotes the target of nucleus (**d**) The cell died and lysed 24 hours after laser irradiation of nucleus. Scale bar, 10 μm.

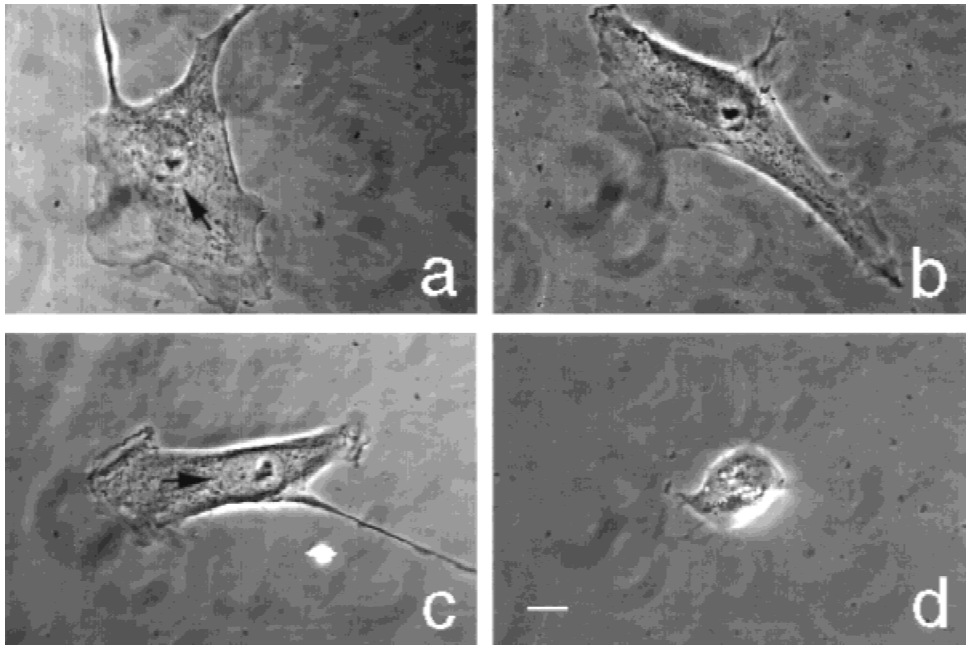

Fig. 10. Cellular damage in PTK_2 cells by pretreated with ALA and laser microirradiation of perinuclear cytoplasm. (**a**) A single cell pretreated with ALA ready to irradiate. Arrow denotes the target of perinuclear cytoplasm. (**b**) The cell remained in healthy condition 24 hours after 30 sec of laser microirradiation. (**c**) Another single cell pretreated with ALA ready to irradiate. Arrow denotes the target of perinuclear cytoplasm. (**d**) The cell died 24 hours later. Scale bar, 10 μm.

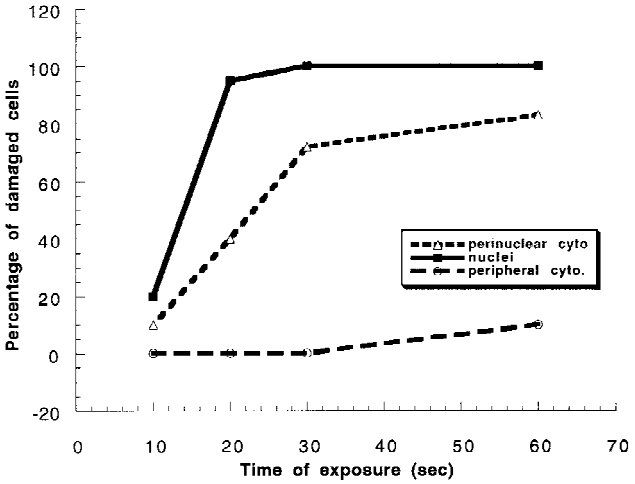

Fig. 11. Cellular toxicity at 24 hours after subcellular laser microirradiation in PTK_2 cells treated with ALA.

cell types no fluorescence was detected in the nucleus despite the fact that a sensitive cooled CCD detector was used. Uberriegler et al. [13] showed that low concentrations of ALA (10–110 μg/ml) led to a bright fluorescing perinuclear region in W138 cells. These findings support the pattern of fluorescence observed in our studies. The results are consistent with our previous work with hematoporphyrin derivative (HPD) which demonstrated a perinuclear pattern of fluorescence, with little or no fluorescence in the peripheral cytoplasm or the nucleus [11]. The present study, coupled with these earlier reports, suggest that ALA induced endogenous protoporphyrin production in bovine artery endothelium cells and PTK_2 cells leads to a fluorescence which is primarily confined to the mitochondria-rich perinuclear cytoplasm.

The phototoxicity studies for both the CPAE and PTK_2 cells demonstrate that the nucleus is the most sensitive region of the cell followed by the perinuclear cytoplasm and the peripheral cytoplasm. However there are distinctive differences in the responses of the two cell types: (1) control nuclear irradiation (light without sensitizer) results in significant toxicity in the CPAE cells and not in the PTK_2 cells, and (2) the total light dose necessary to produce cell damage (in all cell regions) in ALA-treated cells is an order of magnitude (ten-fold) greater in the CPAE cells than in the PTK_2 cells. The first difference may actually be explained by the second difference: 5–10 minutes exposure without any sensitizer (total energy densities of 2.2×10^{10}–4.4×10^{10} $>W/cm^2$) may produce enough cumulative nuclear damage (caused by some heating or accumulation of multiphoton-induced photoproduct) to be toxic to the cell (despite the absence of any known chromophore). That this is a nuclear-specific effect, is suggested by the fact that in both cell types, control light exposures to the perinuclear cytoplasm

TABLE 3. Cell Status Morphologically in PTK_2 After Treatment of ALA Plus Laser Microirradiation

Target of irradiation	Pretreatment of ALA	Time of exposure (sec)	Total no. of cells attempted	Cell status after 24 hours				Cell status after 48 hours			
				Healthy cell[a]		Damaged cell[b]		Healthy cell[a]		Damaged cell[b]	
				No.	%	No.	%	No.	%	No.	%
Nucleus	no	60	9	9	100	0	0	9	100	0	0
	yes	60	10	0	0	10	100	0	0	10	100
	yes	30	19	0	0	19	100	0	0	19	100
	yes	20	21	1	5	20	95	1	5	20	95
	yes	10	10	8	80	2	20	6	60	4	40
	yes	5	9	6	67	3	33	5	56	4	44
Perinuclear cytoplasm	no	300	6	6	100	0	0	6	100	0	0
	yes	300	13	0	0	13	100	0	0	13	100
	no	60	8	8	100	0	0	8	100	0	0
	yes	60	6	1	17	5	83	0	0	6	100
	yes	30	18	5	28	13	72	2	11	16	89
	yes	20	30	18	60	12	40	12	40	18	60
	yes	10	10	9	90	1	10	8	80	2	20
	yes	5	8	6	75	2	25	6	75	2	25
Peripheral cytoplasm	no	300	6	6	100	0	0	6	100	0	0
	yes	300	10	3	30	7	70	2	20	8	80
	yes	60	10	9	90	1	10	8	80	2	20
	yes	30	18	18	100	0	0	16	89	2	11
	yes	10	10	10	100	0	0	10	100	0	0

[a]Healthy cell: Cells underwent at least one additional mitosis and cells with no division but morphologically normal, alive and healthy.
[b]Damaged cell: Cells morphologically aberrant such as with large volume or multi-nuclei and cells vacuolated, disintegrated and lysed.

in non-ALA treated cells (Tables 2 and 3) do not result in any cell damage 48 hours following exposure to 5 minutes of light. However, it is not possible to eliminate totally the possibility that some photosensitizer does penetrate into the nucleus, accounting for a photodynamic response.

Taking into consideration the control light exposure data as well as the ALA/light exposure data and the fluorescence distribution patterns, the PDT mechanism of cell damage appears to be mitochondrial-mediated in the CPAE cells. The high concentration of mitochondria in the perinuclear region is consistent with this hypothesis. Furthermore, considering the amount of toxicity following light exposure to nuclei in control cells, the toxicity of the perinuclear light exposure in the ALA-treated cells is greater. The observations in the PTK_2 cells appear to be different. It is clear from the data that the nucleus is more sensitive than the perinuclear cytoplasm at the light doses used (Table 3). For example at 24 hours following light exposure of 60, 30, 20, 10, and 5 seconds, the percent of damaged cells for nuclear exposure was 100%, 100%, 95%, 20%, and 33%. But for perinuclear exposure to the same light doses, it was 83%, 72%, 40%, 10% and 15%. Thus, even though both regions were sensitive to PDT, the nucleus was more sensitive.

In an effort to understand the nature of the nuclear sensitivity, CPAE cells treated with ALA were exposed to light in the cytoplasm region directly above or below the nucleus. However, because the laser beam was focused to a small 0.5 micron diameter spot in that region, the non-absorbed portion of the beam diverged through its focal point and still exposed the nucleus to light (or vice versa for a beam focused to a focal point on the other side of the nucleus). Because of the high rate of divergence, the energy density (per area and/or volume) in the nucleus was of a much lower value than the energy density at the focal point in the cytoplasm. In this experiment (Table 2) the PDT toxicity was 20% and 30% at 24 and 48 hours after light exposure. This contrasts to 100% toxicity at the same time periods in ALA-treated cells that were exposed to the light directly in the nucleus at the higher energy densities.

Unfortunately, from the preceding experiment it is not possible to determine whether the nuclear toxicity is caused by direct interaction of the light with a small amount of sensitizer that may be in the nucleus, or whether the mitochondria-associated sensitizer releases a photoproduct that has its cytotoxic effect on the nucleus. The reason for this ambiguity is that it is not possible to expose the nucleus to the light without the

beam traversing some perinuclear cytoplasm which, based upon the fluorescence microscopy, is rich in mitochondria. However, the fact that the low light level CCD camera can not detect any fluorescence in the nucleus, strongly suggests that both nuclear and perinuclear phototoxicity are due to photo products associated with the protoporphyrin IX binding to mitochondria which are clustered around the nuclei. Final assessment of the nature of the subcellular toxic effects must await further ultrastructural and biochemical analysis. These studies will permit correlation of microscopic damage with functional alterations.

The differences between the responses of CPAE and PTK_2 cells may be attributed to many factors: different tissue origin, different amounts of sensitizer binding, difference in organelle concentration, basic differences in cell metabolism (CPAE are cells of a low passage number and PTK_2 are an established cell line that has been in culture for over 25 years). Despite these differences, we have demonstrated that ALA and/or its conversion product protoporphyrin IX is localized in mitochondria in the perinuclear region of both bovine vascular endothelium cells (CPAE) and rat kangaroo kidney cells (PTK_2) in vitro. This cell region is particularly sensitive to subcellular light exposure, resulting in PDT-mediated cell toxicity.

ACKNOWLEDGMENTS

We thank Dr. Chung-Ho Sun and Ms. Marie Hammer-Wilson for their suggestions and assistance concerning cell culture and drug treatment, Mr. Jeffrey Andrews for his assistance with laser equipment and Dr. Tatiana B. Krasieva for her assistance with fluorescence microscopy.

This work is sponsored by grants from the National Institutes of Health R01CA32248 and RRO1192, the Office of Naval Research (ONR N00014-91-C-0134), the Department of Energy (DE-F03-91ER61227), and the Beckman Laser Institute Endowment.

REFERENCES

1. Doughty TJ. Photodynamic therapy. Photochem Photobiol 1993; 58:895–900.
2. Schneckenburger H, Konig K, Kunzi-Rapp K, Westphal-Frosch C, Ruck A. Time-resolved in-vivo fluorescence of photosensitizing porphyrins. J Photochem Photobiol B:Biol 1993; 21:143–147.
3. Kennedy JC, Pottier RH. Endogenous protoporphyrin IX, a clinically useful photosensitizer for photodynamic therapy. J Photochem Photobiol B:Biol 1992; 14:275–292.
4. Kennedy JC. ALA-PDT: An overview. Photochem Photobiol Suppl 57., 76s (Abstract) 1993.
5. Charlesworth P, Truscott TG. The use of 5-aminolaevulinic acid (ALA) in photodynamic therapy. J Photochem Photobiol B:Biol 1993; 18:99–100.
6. MIkvy P, Messmann H, Regula J, Conio M, Pauer M, Millson CE, MacRobert AJ, Bown SG. Sensitization and photodynamic therapy (PDT) of gastrointestinal tumors with 5-aminolaevulinic acid (ALA) induced protoporphyrin IX (PPIX). A pilot study. Neoplasma 1995; 42:109–113.
7. Henderson BW, Waldow SM, Mang TS, Potter WR, Malone PB, Doughty TJ. Tumor destruction and kinetics of tumor cell death in two experimental mouse tumors following photodynamic therapy. Cancer Res 1985; 45: 572–576.
8. Nelson JS, Liaw L-H, Berns MW. Tumor destruction in photodynamic therapy. Photochem Photobiol 1987; 46: 829–835.
9. Zhou, C. Mechanisms of tumor necrosis induced by photodynamic therapy. J Photochem Photobiol B:Biol 1989; 3:299–318.
10. He DP, Hamption JA, Keck R, Selman SH. Photodynamic therapy: Effect on the endothelial cell of the rat aorta. Photochem Photobiol 1991; 54:801–804.
11. Berns MW, Dahlman A, Johnson FM, Burns R, Sperling D, Guiltiness M, Siemens A, Walter R, Wright W, Hammer-Wilson M, Wile A. In vitro cellular effects of hematoporphyrin derivative. Cancer Res 1982; 42:2326–2329.
12. Misawa H, Koshioka M, Sasaki K, Kitamura N, Masuhara H. Three dimensional optical trapping and laser ablation of a single polymer latex particle in water. J Appl Phys 1991; 70:3929–3836.
13. Uberriegler KP, Banieghbal E, Krammer B. Subcellular damage kinetics within co-cultivated W138 and VA13-transformed W138 fibroblasts following 5-aminolaevulinic acid-induced protoporphyrin IX formation. Photochem Photobiol 1995; 60:1052–1057.